13

Surface Analysis of Polycrystalline CVD- Diamond after Static Thermochemical Treatment

© A.V. Lebedenko,[1,2] I.V. Klepikov,[1,2,3] E.N. Kulikov,[4] A.V. Deryabkin,[4] Y.Y. Fedorov,[4] V.A. Shepelev,[2] A.A. Altukhov[2]

[1]St. Petersburg State University,
199034, St. Petersburg, Russia
[2]MIREA — Russian
Technological University,
125993 Moscow, Russia
[3]OOO „Scientific Production Complex „Almaz“,
197706 Sestroretsk, St. Petersburg, Russia
[4]AO „Scientific Production Enterprise „Istok“ Named After A.I. Shokin“,
141190 Fryazino, Moscow Oblast., Russia
e-mail: a.lebedenko@spbu.ru

Received October 18, 2024
Revised October 18, 2024
Accepted October 18, 2024

This paper presents a comprehensive surface analysis of polycrystalline CVD-diamond after static thermochemical treatment (TCT). The study focuses on subtle changes in the morphology and surface roughness of the diamond before and after TCT. Optical, atomic force, and scanning electron microscopy methods were used to conduct the analysis, allowing for detailed characterization of both macroscopic and microscopic changes. The results show a reduction in surface roughness parameters, significant changes in surface relief and textures, indicating the effectiveness of TCT for such a complex material as polycrystalline diamond.

Keywords: CVD- diamond, polycrystalline diamond, polycrystal, surface roughness, thermochemical treatment method, thermochemical treatment.

DOI: 10.61011/TP.2025.03.60862.322-24

Introduction

Polycrystalline diamond (PCD) is a material with a very promising combination of physical properties, size (diameter and thickness of wafers for use at existing industrial facilities), and cost. It finds application in semiconductor device structures, optical components, and heat-dissipating and wear-resistant coatings [1–7]. The required processing and polishing of large-diameter (up to 100 mm) PCD wafers, which are produced by the CVD method in order to improve the surface quality, become an important stage of their preparation for efficient application as heat sinks. The subsequent fine polishing process is also very important, since it reduces the surface roughness, which, in turn, affects the thermal contact resistance when a heat sink is mounted on electronic devices [8–10]. Although thermal conductivity is crucial for heat sinks, the anisotropy of thermal conductivity of PCD is also important. This anisotropy of thermal properties further highlights the importance of understanding and optimizing the microstructure in preparation of these materials for use in thermal management systems [10].

Standard mechanical grinding/polishing of PCD often results in surface damage and contamination; the material removal rate is low ($0.1-0.5\,\mu$m/h), and a surface microroughness of about 40 nm may be achieved [11–13]. Final smoothing methods, such as a novel technique for polishing by ultraviolet (UV) irradiation that provides a surface roughness of 0.2 nm at a higher material removal rate [14], are also available. The use of fixed abrasive tools with mechanochemical diamond grains for grinding and polishing of PCD allows one to produce mirror surfaces (through to 40 nm), especially when such processing is performed with the use of SiO_2 at high temperatures [15]. „Dry“ polishing, which relies on such thermochemical reactions as graphitization and oxidation, has also been attempted (the resulting roughness was 40–60 nm) [16]. The efficiency of a method combining diffusion treatment and milling with a free abrasive has been demonstrated in [17]. Other methods include the use of various polishing pastes and disks [18]. Laser processing has also been proposed: a low-energy fiber laser enhances hardness and maintains surface roughness by inducing plastic deformation of grains and altering the area of intercrystalline interfaces [19,20]. Various PCD processing methods are available, each with its own advantages. A specific technique is chosen based on the initial surface roughness parameters, surface finish requirements, and the nature of the PCD- material being processed. Methods are combined, improved, and used conjointly when necessary.

Thermochemical treatment (TCT) is one of the promising methods for processing polycrystalline CVD- diamond. This method is aimed at improving the mechanical properties

of the diamond surface by eliminating internal stresses and defects [21]. It has been first applied to CVD- diamond films in the early 1990s [22]. The process involves pressing diamond against a catalytic metal (such as iron, nickel, manganese, or molybdenum) plate heated to 730−900°C. A diamond sample may either remain static or move relative to the plate (at low velocities and pressure). At high temperatures, the metal in contact with diamond acts as a catalyst, lowering the activation energy for conversion of diamond into non-diamond carbon. Non-diamond carbon is then removed from the diamond surface by diffusion into the metal plate. The conversion, diffusion, and polishing rates increase exponentially with temperature, contact pressure, and transverse vibration amplitude [23]. The process is inefficient at low temperatures, while high temperatures may lead to etching and pitting (especially when oxygen is present) [24]. TCT at 1000−1100°C made it possible to achieve a roughness of about 0.8 μm at a grinding rate varying from 20 μm/h to 3 mm/h [25]. Thermal etching, wherein iron is substituted with elements with a higher carbon solubility [26], is a special type of TCT and polishing. At a temperature of 900°C in argon atmosphere, carbon diffuses into manganese powder, foil, or patterned thin film that are in contact with the diamond surface. The choice of metal is of key importance in this case. For example, pure Ce used at a temperature of 700°C provides a very high material removal rate (more than 25 μm/h), but the resulting average surface roughness remains at the micrometer level [27,28].

One research group has performed a dry PCD grinding test using a PCD- disc as a grinding tool. It was found that thermochemical reactions may affect the roughness of the ground face: an increase in electronegativity resulted in a rougher surface due to weakening of covalent bonds in diamond [29]. However, more detailed data on the initial crystallite sizes and roughness values after grinding have not been provided. Another research group has presented a technology for processing diamond substrates with the use of an iron plate and a hydrogen peroxide solution (H_2O_2). This method utilizes hydroxyl radicals (IOH-radicals) formed as a result of decomposition of H_2O_2 on the surface of iron to produce an atomically smooth diamond surface [30]. A method of thermochemical post-processing aimed at improving the mechanical properties of mechanically polished diamond crystals is also known. It allows one to eliminate internal stresses and defects induced by mechanical actions in the damaged surface layer of the material [31]. In addition, the quality of PCD- structures, which depends on the concentration of defects (such as grain boundaries and impurities), is a key factor governing the efficiency and outcome of grinding [31–36].

In the present study, the surface morphology of three CVD PCD samples $\sim 5 \times 5$ mm in size was examined with an atomic force microscope (AFM) before and after static TCT. The aim was to characterize in detail the quality of the original and processed surfaces. The selection of optimum parameters of surface roughness of heat-dissipating PCD-elements and their processing is a relevant applied problem.

1. Objects and methods of study

Three samples of polycrystalline CVD- diamond (typical of the production of heat-dissipating elements of semiconductor device assemblies) provided by JSC „Scientific Production Enterprise „Istok“ Named After A.I. Shokin,“ which serve as illustrative examples, were studied. Sample No. 2 is an example of the surface of an untreated polycrystalline diamond wafer (sample dimensions: $3.31 \times 3.78 \times 0.21$ mm). Samples Nos. 1 and 3, which are illustrative of the technological process of batch production of heat-dissipating elements of semiconductor device assemblies, were made from a single CVD- PCD wafer and subjected to TCT in use at JSC „Scientific Production Enterprise „Istok“ Named After A.I. Shokin.“ The dimensions of samples Nos. 1 and 3 are $9.57 \times 5.25 \times 0.19$ and $3.05 \times 3.49 \times 0.10$ mm, respectively. Static TCT was carried out in a hydrogen furnace at a temperature around 1100°C on a nickel plate of surface finish grade 9. This processing method allows one to obtain a surface roughness of polycrystalline CVD- diamond of less than 1 μm; the material removal rate is 30−50 μm/h [37]. This TCT type is a variation of grinding (i.e., a rough surface preparation procedure). In addition to reducing surface roughness, it provides significant leveling of the surface of polycrystalline diamond samples. The samples were imaged with a Leica M205 C stereomicroscope. A Quanta 200 3D multifunctional scanning electron microscope with an integrated focused ion beam system was used to perform an in-depth study of the surface features of polycrystals. The structural features of the sample surface were examined using an atomic force microscope (INTEGRA-AURA probe nanolaboratory). These experiments were conducted at the Centre for Microscopy and Microanalysis (St. Petersburg State University).

2. Results

2.1. Polycrystalline diamond prior to TCT

The morphology of CVD PCD prior to TCT (sample No. 2) is represented by a complex aggregate consisting of octahedral habit crystallites up to 0.05 mm in size (Fig. 1, *a*). The distribution of crystallites on the surface of the sample is non-uniform: a small depression of an isometric shape is present at the center of the wafer. Parallel elongated zones of elevated crystallites are also seen. Larger octahedral crystallites (up to 0.1 mm in size), which form a small step, are found along the periphery of the wafer (Fig. 1, *b*).

Backscattered electron images make it clear that the crystallites of sample No. 2 have a sharp-edged octahedral habit and are 10−50 μm in size. Parallel elevated elongated zones are distinguished most clearly (Fig. 2, *a*). The relief is

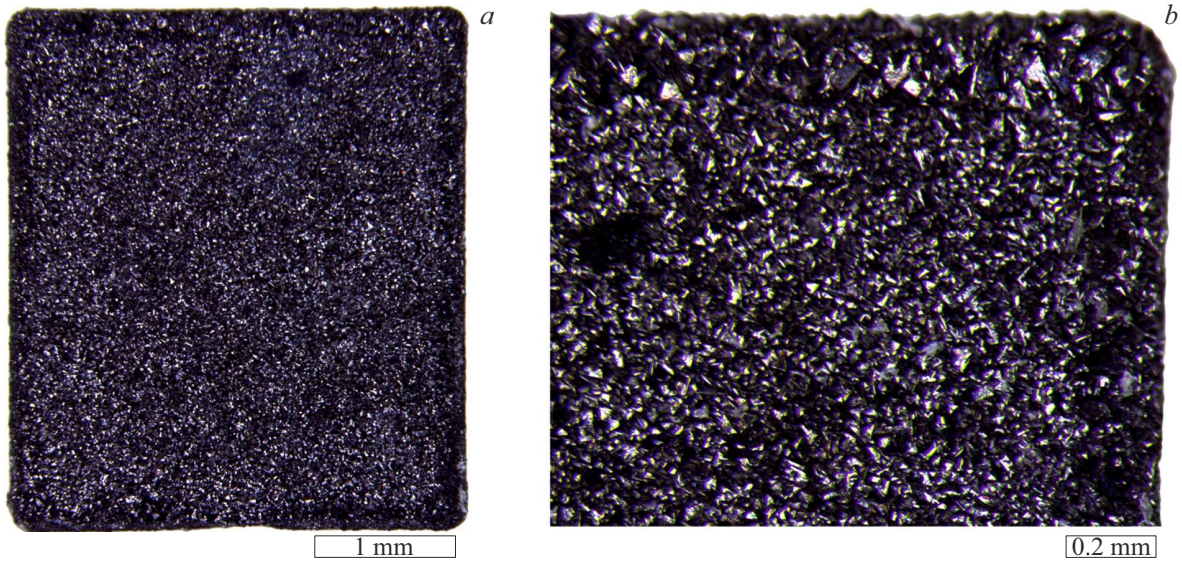

Figure 1. Optical microscopic images of PCD prior to TCT: *a* — overall view of sample No. 2; *b* — enlarged corner fragment of a section of sample No 2.

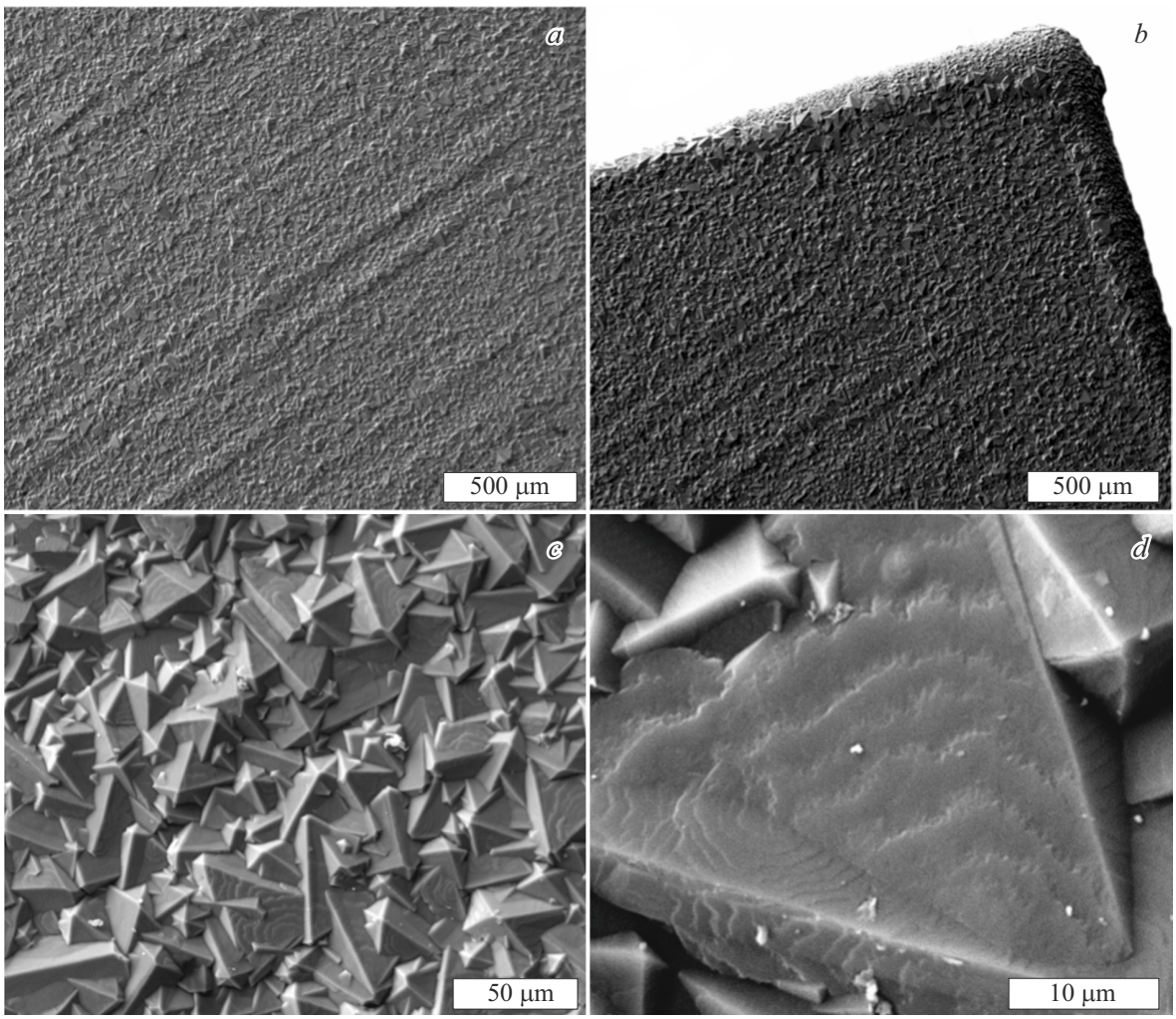

Figure 2. Backscattered electron images of CVD PCD prior to TCT: *a* — fragment of the central region of sample No. 2, *b* — enlarged fragment of the edge of sample No. 2, *c* — enlarged fragment of the central region of sample No. 2, and *d* — lamellar-stepped concentric-zonal structure of the octahedral crystallite face of sample No 2.

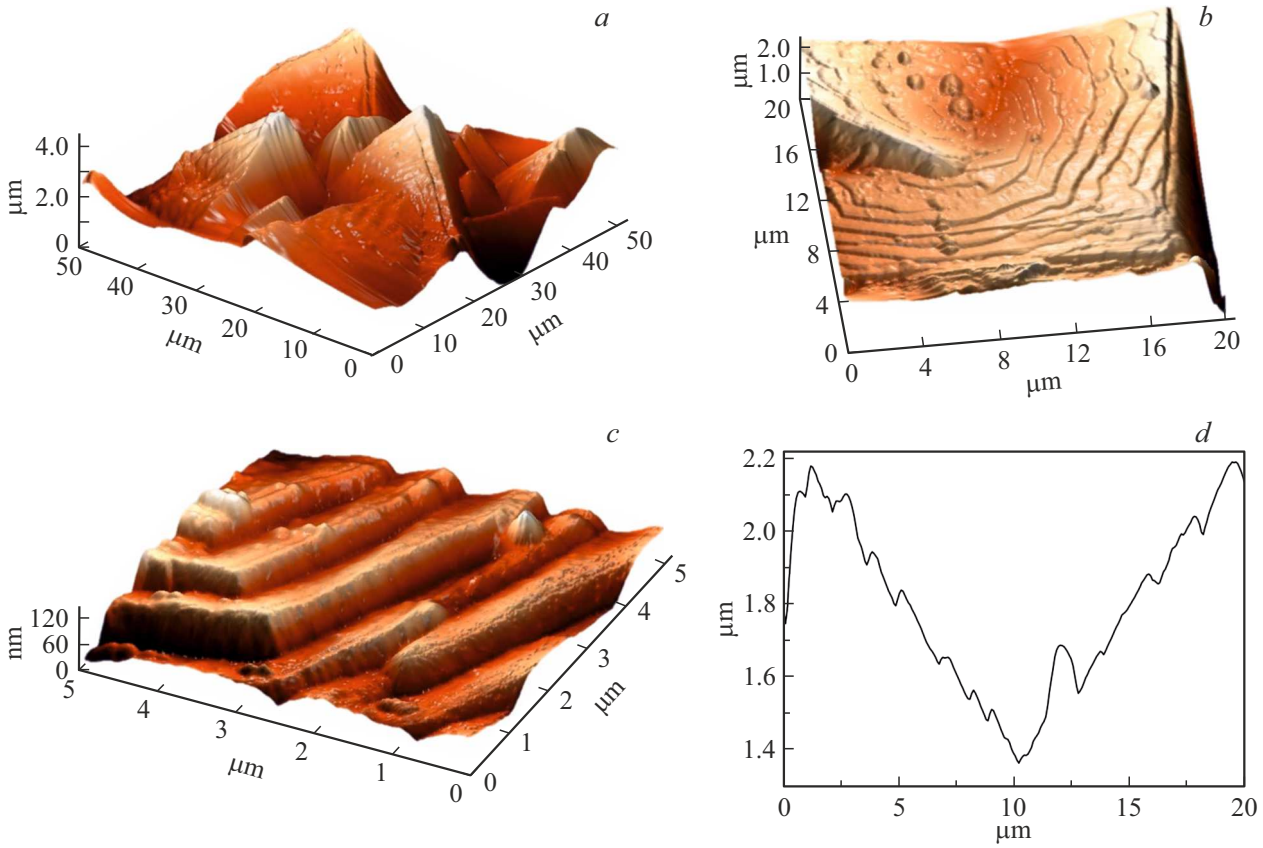

Figure 3. AFM images of CVD PCD prior to TCT: *a* — 3*D*-image of octahedral crystallites from the central region of sample No. 2; *b* — 3*D*-image of the lamellar-stepped concentric-zonal structure of the octahedral crystallite face of sample No 2; *c* — 3*D*-image of a fragment of the octahedral crystallite face; *d* — longitudinal profile of region *b*.

elevated on the edges of the wafer (Fig. 2, *b*); at the ends of the sample, the crystallites are significantly smaller (down to 10 μm). Twin fragments (penetration twins) are revealed under high magnification (Figs. 2, *c, d*). The octahedral faces of crystallites have a lamellar-stepped concentric-zonal structure (Figs. 2, *c, d*).

AFM studies demonstrated that the height of octahedral CVD PCD crystallites reaches 6 μm (Fig. 3, *a*) prior to TCT, and they have a pronounced lamellar-stepped structure. A distinct concentric-zonal layering of lamellae was revealed under higher magnification (Fig. 3, *b*). The height difference between the steps is 0.1–0.3 μm. The steps themselves are inclined to the horizontal plane (Figs. 3, *c, d*). The ends of steps are also inclined to the vertical plane (Figs. 3, *c, d*). Surface roughness Ra of this sample within a 100 × 100 μm region is $\sim$ 2 μm; in certain regions, it reaches 20 μm.

2.2. Polycrystalline diamond after TCT

Optical microscope images of samples Nos. 1 and 3 of polycrystalline diamond after TCT are shown in Fig. 4. They are characterized by a macroscopically smooth surface with mild striation and texturing (Figs. 4, *b, d*). A rough surface and small round pits (in certain regions) were revealed under high magnifications (Figs. 4, *b*). A slight inclination of the plane of sample No. 3, which is especially noticeable in the central part of the wafer, was observed after TCT.

Examined with a scanning electron microscope, samples Nos. 1 and 3 subjected to TCT revealed clearly defined parallel striations (Figs. 5, *a, b*). Their surface relief is heterogeneous: it features small hillocks and pits, as well as zones with a cellular structure. Octahedral crystallites were not observed. Under high magnifications, the microporous structure of PCD after TCT (Fig. 5, *c*) and small round smoothed hillocks (Fig. 5, *d*) are discernible.

Atomic force microscopy studies revealed that round hillocks, which occasionally reach a height of 4 μm, are the dominant feature of surface relief (Fig. 6, *a*). Large hillocks of the micro-rough surface (Fig. 6, *b*) are formed from a large number of smaller hillocks (Figs. 6, *c, d*). The differences in height between large hillocks are 1–2 μm. Surface roughness Ra is close to 500 nm; this value is reproduced in different regions.

3. Discussion

The results of optical, electron, and atomic force microscopy studies revealed that the examined CVD PCD

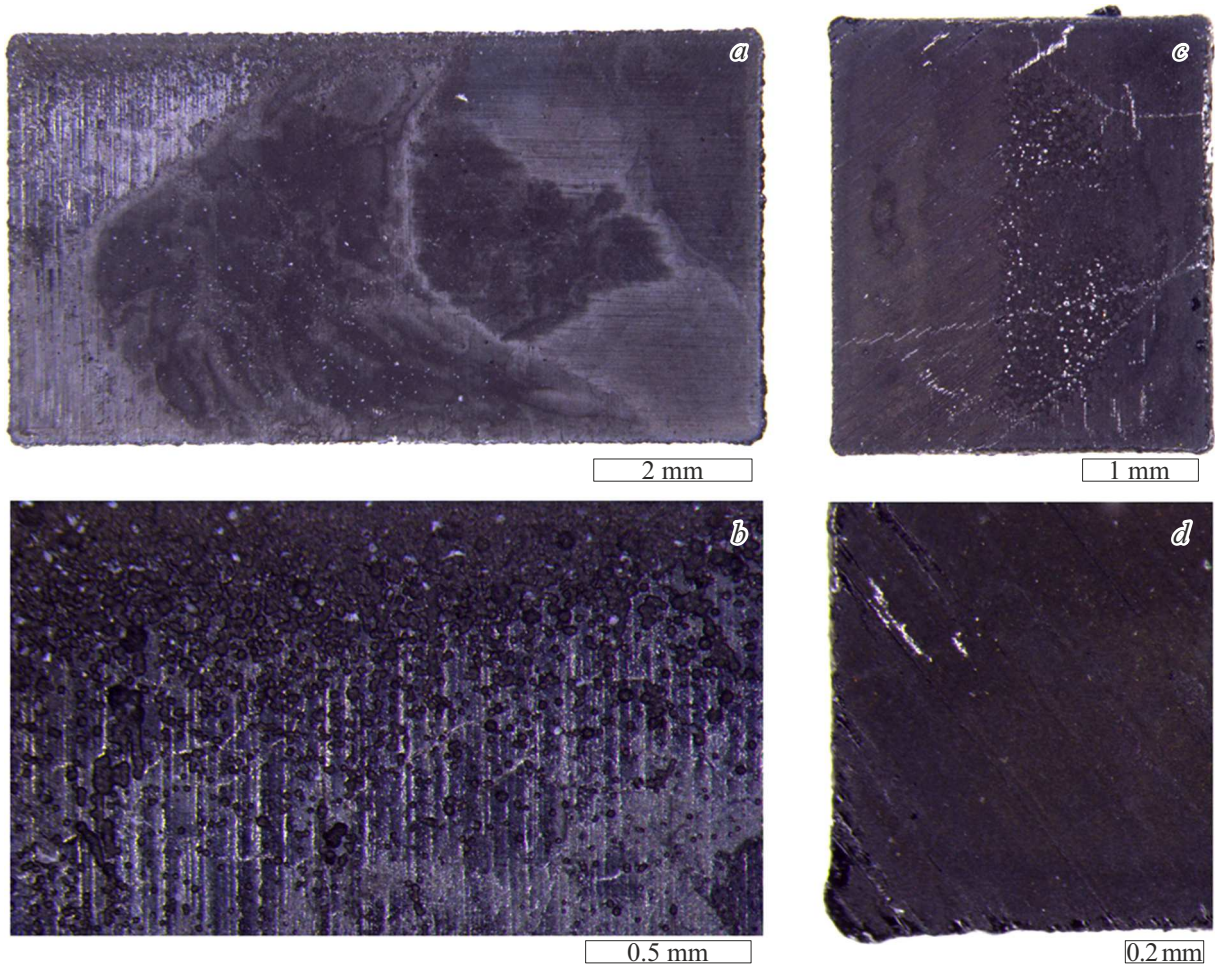

Figure 4. Optical microscope images of CVD PCD after TCT: *a* — overall view of sample No. 1; *b* — enlarged fragment of sample No. 1; *c* — overall view of sample No.. 3; *d* — enlarged fragment of sample No.. 3.

Summary results of the study of surface roughness and maximum height differences

No.	Region	Region size, μm	Surface roughness Ra, nm	Maximum height difference, μm
2	1	100 × 100	627.3	5.0
	2	100 × 100	1251.9	5.0
	3	50 × 50	682.1	4.0
	4	20 × 20	338.9	3.0
	5	20 × 20	148.0	2.3
1	1	100 × 100	418.5	2.5
	2	100 × 100	450.4	2.5
	3	50 × 50	426.1	2.5
	4	20 × 20	338.4	2.0
	5	5 × 5	170.1	0.9
3	1	100 × 100	595.4	2.5
	2	100 × 100	187.4	2.0
	3	50 × 50	585.6	2.0
	4	20 × 20	216.0	1.4

samples used as heat-dissipating elements consist of octahedral crystallites with a stepped structure of faces, are characterized by the presence of penetration twins, and have a surface roughness of 600–2000 nm prior to TCT.

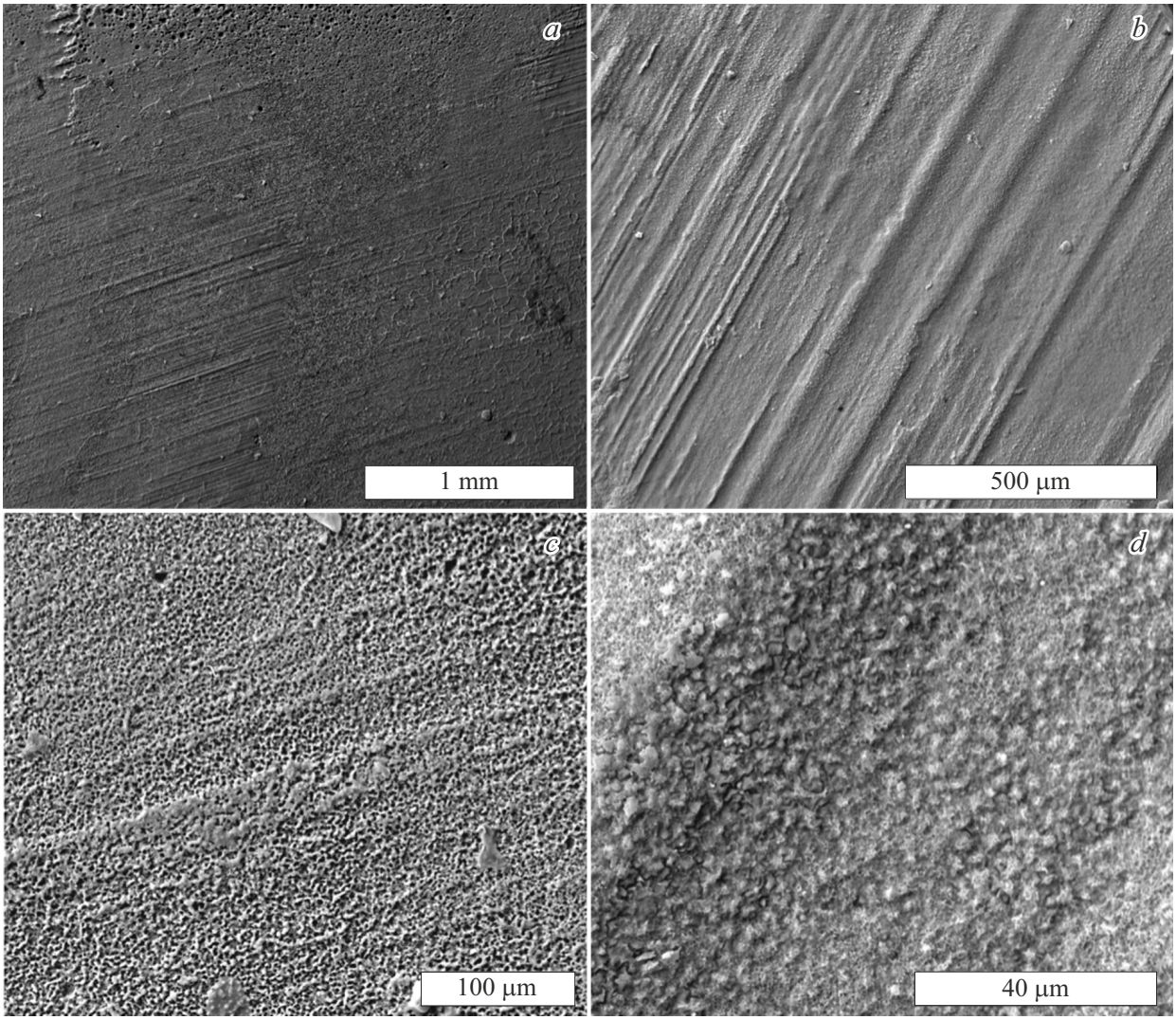

Figure 5. Backscattered electron images of CVD PCD after TCT: *a, b* — fragments of the central regions of samples No.s. 1 and 3, respectively; *c* — enlarged fragment of the central region of sample No. 1 with a cellular structure; *d* — enlarged fragment of the central region of sample No. 3 with hillocks and depressions.

The samples after TCT have a roughness of 170–600 nm; octahedral crystallites are rounded completely over the entire surface and are transformed into smoothed round hillocks. The maximum height difference was 2.3–5.0 μm for sample No. 2 (prior to TCT) and 0.9–2.5 μm for the samples after TCT. The results of examination of surface roughness and maximum height differences are presented in the table.

The static TCT method allows one to reduce the roughness of a complex surface of polycrystalline diamond that is virtually impervious to standard mechanical processing. However, the results of optical and electron microscopy are indicative of certain non-uniformity of processing: the surfaces of CVD PCD samples after TCT are characterized by the presence of hillocks and depressions, zones with a cellular structure, and pores, and parallel striation is clearly visible. The surface roughness differs from one region of the sample to another, but does so within the established limits.

Thus, it was demonstrated clearly that the methods of optical, atomic force, and scanning electron microscopy provide an opportunity to characterize PCD surfaces of different quality and identify their defects within a wide range of magnitudes. Static TCT is a promising method for reducing the surface roughness of PCD. The procedure of TCT of large PCDs ($d \geq 100$ mm) requires further improvement, and a subsequent stage of thermochemical polishing needs to be introduced in order to reduce the level of surface roughness of heat-dissipating elements to tens of nanometers (with surface inspection by the methods used in the present study). The mechanism of PCD- surface smoothing is the transformation/dissolution of sharp-edged octahedral crystallites into round hillocky surfaces that, in turn, are formed by smaller hillocks.

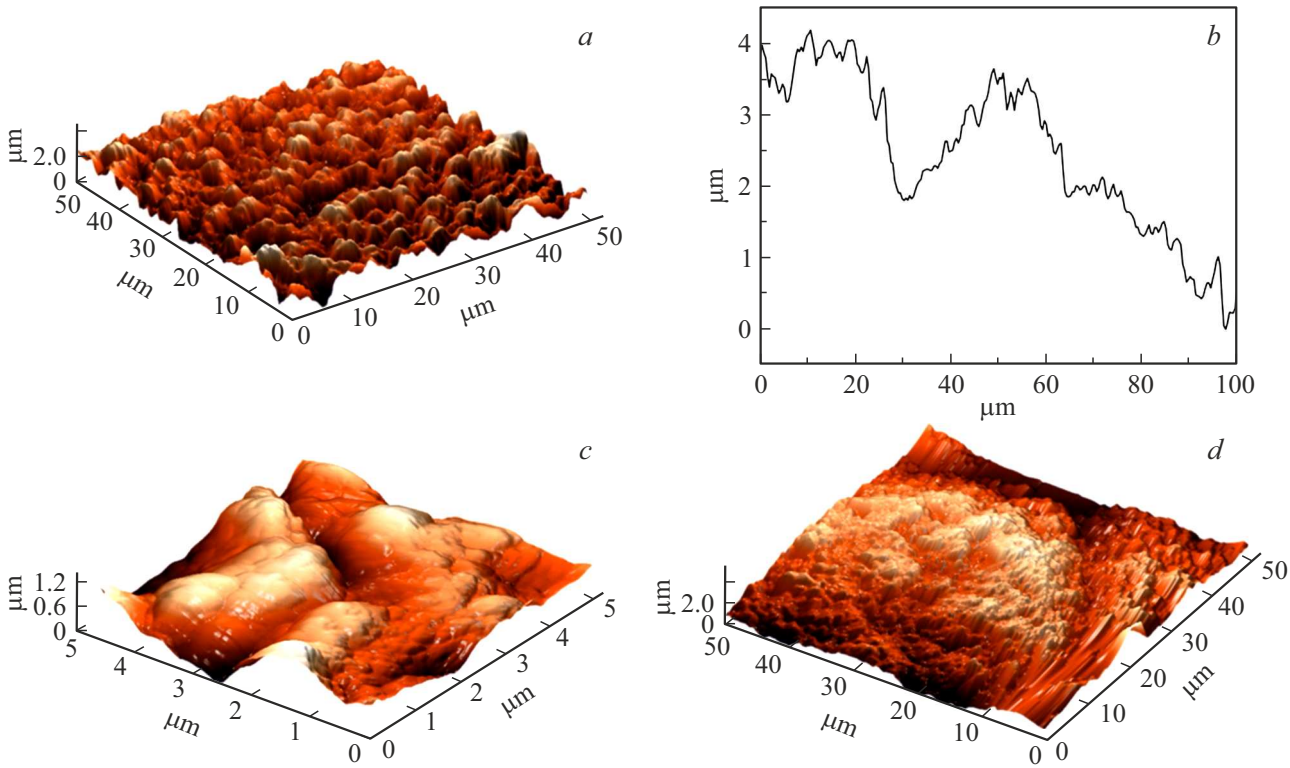

Figure 6. Atomic force microscope images of CVD PCD after TCT: *a* — 3*D*-image of sample No. 3 with its surface formed by round hillocks; *b* — longitudinal profile of the region in panel *a*; *c, d* — 3*D*-images of the surface of a large round hillock.

Funding

This study was carried out under the state assignment of the Ministry of Science and Higher Education of the Russian Federation (project No. FSFZ-2022-0006).

Conflict of interest

The authors declare that they have no conflict of interest.

References

[1] R.A. Khmel'nitskii, N.Kh. Talipov, G.V. Chucheva. *Sintetich-eskii almaz dlya elektroniki i optiki* (IKAR, M., 2017) (in Russian).
[2] M. Kim, J.-H. Seo, U. Singisetti, Z. Ma. J. Mater. Chem. C, **5**, 45 (2017). DOI: 10.1039/C7TC02221B
[3] A. Bindra. IEEE Power Electron Magazine, **2** (1), 5 (2015). DOI: 10.1109/MPEL.2014.2382195
[4] S. Fujita. Jpn. J. Appl. Phys., **54** (3), 12 (2015). DOI: 10.7567/JJAP.54.030101
[5] J. Canas, A.C. Pakpour-Tabrizi, T. Trajkovic, F. Udrea, D. Eon, E. Gheeraert, R. Jackman, A.C. Pakpour-Tabrizi, R.B. Jackman. IEEE Trans Electron Devices, **68**, 6 (2021). DOI: 10.1109/TED.2021.3117237ï
[6] Q. He, J. Zhang, Z. Ren, J. Zhang, K. Su, Y. Lei, D. Ly, T. Mi, Y. Hao. Diamond Related Mater., **119**, 5 (2021). DOI: 10.1016/j.diamond.2021.108547
[7] T. Matsumoto, T. Yamakawa, H. Kato, T. Makino, M. Ogura, X. Zhang, T. Inokuma, S. Yamasaki, N. Tokuda. Appl. Phys. Lett., **119**, 5 (2021). DOI: 10.1063/5.0075964
[8] P.L. Tso, T.M. Wang. Adv. Mater. Res., **76–78**, 6 (2009). DOI: 10.4028/www.scientific.net/AMR.76-78.207
[9] P.P. Mal'tsev, S.V. Red'kin, I.A. Glinskii, N.V. Poboikina, M.P. Dukhnovskii, Yu.Yu. Fedorov, A.K. Smirnova, E.N. Kulikov, S.V. Shcherbakov, I.A. Leont'ev, O.Yu. Kudryashov, A.S. Skripnichenko. Nano- Mikrosist. Tekh., **18** (4), 13 (2016) (in Russian).
[10] H.Y. Tsai, C.J. Ting, C.P. Chou. Diamond Related Mater., **16**, 9 (2007). DOI: 10.1016/j.diamond.2006.06.007
[11] T. Schuelke, T.A. Grotjohn. Diamond Related Mater., **32**, 10 (2013). DOI: 10.1016/j.diamond.2012.11.007
[12] L. Zhang, D.H. Wen, S.M. Ji, Q.L. Yuan, Z.H. Xu. Adv. Mater. Res., **69–70**, 7 (2009). DOI: 10.4028/www.scientific.net/AMR.69-70.192
[13] C.H. Hsieh, H.Y. Tsai, H.T. Lai, H.Y. Lin. Nano- and Microtechnology: Mater., Processes, Packaging, Systems, **4936**, 8 (2002). DOI: 10.1117/12.469741
[14] J. Watanabe, M. Touge, T. Sakamoto. Diamond Related Mater., **39**, 6 (2013). DOI: 10.1016/j.diamond.2013.07.001
[15] K. Yamaguchi, M. Ota, K. Egashira, H. Miwa, Y. Onchi, K. Tanada. Trans Tech. Publications, **874**, 6 (2016). DOI: 10.4028/www.scientific.net/MSF.874.139
[16] T. Kuriyagawa, K. Syoji. *Progress in Precision Engineering* (Springer, Berlin, 1991) DOI: 10.1007/978-3-642-84494-2_47
[17] Z.M. Cui, Y.G. Han, J.P. Kong, Q.Q. Chen. Adv. Mater. Res., **797**, 5 (2013). DOI: 10.4028/www.scientific.net/AMR.797.491
[18] M.J. Ashe, G.A. Tripp, F.C. Eichmiller, L.A. George, J.C. Meiers. JADA, **127**, 6 (1996). DOI: 10.14219/jada.archive.1996.0059
[19] M. Pacella. Procedia CIRP, **87**, 5 (2020). DOI: 10.1016/j.procir.2020.02.084

[20] F.Y. Chang, C.F. Hsu, W.H. Lu. Appl. Sci., **11** (5871), 22 (2021). DOI: 10.3390/app11135871
[21] M.G. Warhanek, J. Pfaff, L. Meier, C. Walter, K. Wegener. SPIE Proceed., **9736**, 10 (2016). DOI: 10.1117/12.2212771
[22] A.V. Deryabkin, Yu.Yu. Fedorov, M.P. Temiryazeva. VII Vserossiiskaya nauchno-tekhnicheskaya konferentsiya „Elektronika i mikroelektronika SVCh,“ **1**, 1 (2018) (in Russian).
[23] A. Hirata, H. Tokura, M. Yoshikawa. Thin Solid Films, **212**, 6 (1992). DOI: 10.1016/0040-6090(92)90498-z
[24] J.A. Weima, W.R. Fahrner, R. Job. J. Solid State Electrochem., **5**, 7 (2001). DOI: 10.1007/s100080000118
[25] S.A. Eremin, A.M. Kolesnikova, I.A. Leontiev, V.N. Anikin, O.Yu. Kudryashov, Y.M. Yashnov, M.V. Zhdanova. IOP Conf. Ser.: Mater. Sci., **848**, 012016 (2020). DOI: 10.1088/1757-899X/848/1/012016
[26] A.P. Malshe, B.S. Park, W.D. Brown, H.A. Naseem. Diamond Related Mater., **8**, 16 (1999). DOI: 10.1016/s0925-9635(99)00088-6
[27] S. Jin, J.E. Graebner, T.H. Tiefel, G.W. Kammlott, G.J. Zydzik. Diamond Related Mater., **1** (9), 5 (1992). DOI: 10.1016/0925-9635(92)90116-6
[28] M. McCormack, S. Jin, J.E. Graebner, T.H. Tiefel, G.W. Kammlott. Diamond Related Mater., **3**, 5 (1994). DOI: 10.1016/0925-9635(94)90088-4
[29] Z. Minglong, X. Yiben, W. Linjun, S. Hujiang. Solid State Commun., **130**, 4 (2004). DOI: 10.1016/j.ssc.2004.01.013
[30] T. Semba, S. Ohta, Y. Amamoto, H. Fujiyama, H. Sumiya. Transactions Jpn. Society Mechan. Eng., **77** (784), 14 (2011). DOI: 10.1299/kikaic.77.4704
[31] A. Kubota, S. Nagae, S. Motoyama, M. Touge. Diamond Related Mater., **60**, 5 (2015). DOI: 10.1016/j.diamond.2015.10.026
[32] Y. Sun, S. Wang, S. Tian, Y. Wang. Diamond Related Mater., **15**, 6 (2006). DOI: 10.1016/j.diamond.2005.10.057
[33] J.E. Graebner, S. Jin, G.W. Kammlott, B. Bacon, L. Seibles, W. Banholzer. J. Appl. Phys., **71** (5353), 4 (1992). DOI: 10.1063/1.350553
[34] P. Miranzo, M.I. Osendi, E. Garcia, A.J.S. Fernandes, V.A. Silva, F.M. Costa, R.F. Silva. Diamond Related Mater., **11**, 5 (2002). DOI: 10.1016/s0925-9635(02)00028-6
[35] P. Niedermann, W. Hänni, N. Blanc, R. Christoph, J. Burger. J. Vacuum Sci. Technol. A, **14** (1233), 5 (1996). DOI: 10.1116/1.580273
[36] M. Hoinkis, E.R. Weber, M.I. Landstrass, M.A. Plano, S. Han, D.R. Kania. Appl. Phys. Lett., **59** (1870), 2 (1991). DOI: 10.1063/1.106172
[37] A.V. Deryabkin, E.N. Kulikov, A.K. Smirnova. V Vserossiiskaya nauchno-tekhnicheskaya konferentsiya „Elektronika i mikroelektronika SVCh,“ **2**, (2016).

Translated by D.Safin